Correlation Between the Morphology and Dynamic Mechanical Properties of Ethylene Vinyl Acetate/Linear Low-Density Polyethylene Blends: Effects of the Blend Ratio and Compatibilization

K. A. Moly,[1] S. S. Bhagawan,[2] G. Groeninckx,[3] S. Thomas[4]

[1]*Bishop Kurialacherry College, Amalagiry P.O., Kottayam 686036, Kerala, India*
[2]*Department of Polymer Engineering, Amrita Viswa Vidya Peetham, Ettimadai, Coimbatore 641105, India*
[3]*Lab Macromol Struct Chem, Dept Chem, Katholieke Univ Leuven, Celestijnenlaan 200F, B-3001 Heverlee, Belgium*
[4]*School of Chemical Sciences, Mahatma Gandhi University, Priyadharshini Hills P. O., Kottayam 686560, Kerala, India*

Received 28 April 2004; accepted 16 March 2005
DOI 10.1002/app.22466
Published online in Wiley InterScience (www.interscience.wiley.com).

ABSTRACT: The effects of the blend composition and compatibilization on the morphology of linear low-density polyethylene (LLDPE)/ethylene vinyl acetate (EVA) blends were studied. The blends showed dispersed/matrix and cocontinuous phase morphologies that depended on the composition. The blends had a cocontinuous morphology at an EVA concentration of 40–60%. The addition of the compatibilizer first decreased the domain size of the dispersed phase, which then leveled off. Two types of compatibilizers were added to the polymer/polymer interface: linear low-density polyethylene-*g*-maleic anhydride and LLDPE-*g* phenolic resin. Noolandi's theory was in agreement with the experimental data. The conformation of the compatibilizer at the blend interface could be predicted by the calculation of the area occupied by the compatibilizer molecule at the interface. The effects of the blend ratio and compatibilization on the dynamic mechanical properties of the blends were analyzed from −60°C to +35°C. The experiments were performed over a series of frequencies. The area under the curve of the loss modulus versus the temperature was higher than the values obtained by group contribution analysis. The loss tangent curve showed a peak corresponding to the glass transition of EVA, indicating the incompatibility of the blend system. The damping characteristics of the blends increased with increasing EVA content because of the decrease in the crystalline volume of the system. Attempts were made to correlate the observed viscoelastic properties of the blends with the morphology. Various composite models were used to model the dynamic mechanical data. Compatibilization increased the storage modulus of the system because of the fine dispersion of EVA domains in the LLDPE matrix, which provided increased interfacial interaction. Better compatibilization was effected at a 0.5–1% loading of the compatibilizer. This was in full agreement with the dynamic mechanical spectroscopy data. © 2006 Wiley Periodicals, Inc. J Appl Polym Sci 100: 4526–4538, 2006

Key words: blends; compatibilization; glass transition; morphology

INTRODUCTION

Linear low-density polyethylene (LLDPE) is widely used in many consumer and engineering applications. Improving the properties of LLDPE through blending with other polymers can extend the areas of application. Several studies have been reported on the modification of polyethylene with rubbers and plastics. Blends of polyethylene have gained much attention because they possess high processing characteristics and mechanical properties.[1]

Dynamic mechanical analysis (DMA) at a selected fixed frequency over a range of temperatures has grown as a useful analytical technique for the characterization of polymeric mateials—homopolymers, copolymers, blends, and composites—and their evaluation for consideration in stress- and safety-sensitive applications.[2–4] DMA is a technique that helps us to evaluate the glass-transition temperature (T_g) of the blends and the individual components, from which we can assess the miscibility of the blends. The dynamic mechanical properties, such as the storage modulus (E'), loss modulus (E''), and loss tangent (tan δ), of polymer blends depend on the structure, crystallinity, extent of crosslinking,[5] and so forth. The data and information generated may then be employed as a means of fingerprinting polymer systems and for locating glass transitions and associated features. The dynamic mechanical properties of blends of LLDPE and ethylene–propylene–butene-1 terpolymer were studied by Cho et al.[6] The α, β, and γ relaxations, which arise because of the constituents, indicate that the blend is immiscible in the amorphous and crystal-

Correspondence to: S. Thomas (sabut@sancharnet.in or sabut552001@yahoo.com).

TABLE I
Details of the Materials Used

Material	Characteristics	Procured from
LLDPE (Reclair F19010)	Grade: F19010 Melt flow index (g/10 min): 0.9 Density (g/cc): 0.92	Reliance Industries, Ltd. (Hazira, Gujarath, India)
Poly(ethylene-*co*-vinyl acetate) (Piolene 1802)	Vinyl acetate (%): 18 Melt flow index (g/10 min): 2.00 Intrinsic viscosity (dL/g): 0.17 Density (g/cc): 0.937	Polyolefins Industries, Ltd. (Chennai, India)

line phases. Wippler[7] reported on the dynamic mechanical properties of polycarbonate/polyethylene blends and used the Takayanagi model to predict the behavior of experimental E'.

The miscibility and phase behavior of polymer blends is of crucial importance in many applications. The effects of compatibilization on the dynamic mechanical properties of various polymer blends have been reported. An analysis of the data of the dynamic mechanical properties and impact properties for various compositions of elastomer-modified polypropylene blends has revealed a direct correlation between the impact properties and dynamic mechanical loss tangent.[8]

The dynamic mechanical behavior of various thermoplastic elastomer blends was recently reported by this laboratory. Oommen et al.[9] at this laboratory studied the effect of natural rubber-*g*-poly(methyl methacrylate) on the dynamic mechanical and thermal properties of natural rubber/poly(methyl methacrylate) blends. The effects of the compatibilizer loading on E', E'', and tan δ at different temperatures and at different frequencies were analyzed. The dynamic mechanical properties of isotactic polypropylene/nitrile rubber blends were investigated by George et al.[10] Many researchers[11–14] have used DMA to evaluate the compatibility, T_g, phase behavior, and other properties of polymer blends. DMA at the submicrometer scale has also been used for analysis.[15] Miscibility studies on radiation-crosslinked ethylene vinyl acetate (EVA)/LLDPE blends have been performed with temperature-modulated differential scanning calorimetry.[16]

Blends of LLDPE with EVA have advantages of low cost, low density, and ease of processing. They combine the mechanical properties of LLDPE and the flexibility and environmental stress crack resistance of EVA. Earlier, the melt flow behavior and melt elasticity of these blends were reported.[17,18] A thorough examination of the recent literature clearly shows that these blends have tremendous applications in a variety of fields, which include damping applications, outdoor uses, and dielectric applications. However, no detailed analyses have been made until now on the interrelationships of the morphology, dynamic mechanical properties, and compatibilization.

In this article, we report on the morphology and dynamic mechanical properties of LLDPE/EVA blends. The effects of the blend ratio and compatibilization with maleic- and phenolic-modified compatibilizers on the morphology and dynamic mechanical properties have been studied. The area occupied by the compatibilizer in the blend interface has been investigated with a view toward suggesting a possible conformation for the compatibilizer in the interface. Attempts have been made to correlate the dynamic mechanical properties with the morphology of the blend. Finally, the experimental dynamic mechanical properties have been compared with theoretical models.

EXPERIMENTAL

Materials and blend preparation

Details of the polymer [a butene comonomer based LLDPE (Reclair F19010) and EVA (Piolene 1802) with a vinyl acetate concentration of 18%] are given in Table I. The compatibilizer maleic anhydride-*g*-linear low-density polyethylene (MA-*g*-LLDPE) was prepared by the melt mixing of LLDPE (100 parts) with maleic anhydride (MA; 5 parts) and benzoyl peroxide (0.5 g)[19] at 125°C. The phenolic-modified compatibilizer was prepared by the mixing of LLDPE (100 parts) with phenolic resin (4 parts) and stannous chloride (0.8 g) at 125°C. The mixing time was 6 min.

The LLDPE/EVA blends were prepared in a Brabender plasticorder at 125°C at a rotor speed of 60 rpm. LLDPE was first melted for 2 min, and then EVA was added and mixed for 4 min. The total mixing time was 6 min in all cases. The different compositions

TABLE II
T_g of EVA Phases from the Tan δ Curve and E'' Curve

Sample	T_g (°C) from Tan δ curve	T_g (°C) from E'' curve
E_{100}	−11.9	−21.9
E_{70}	−1.2	−7.95
E_{50}	−3.9	−8.3
E_{30}	−5	−9

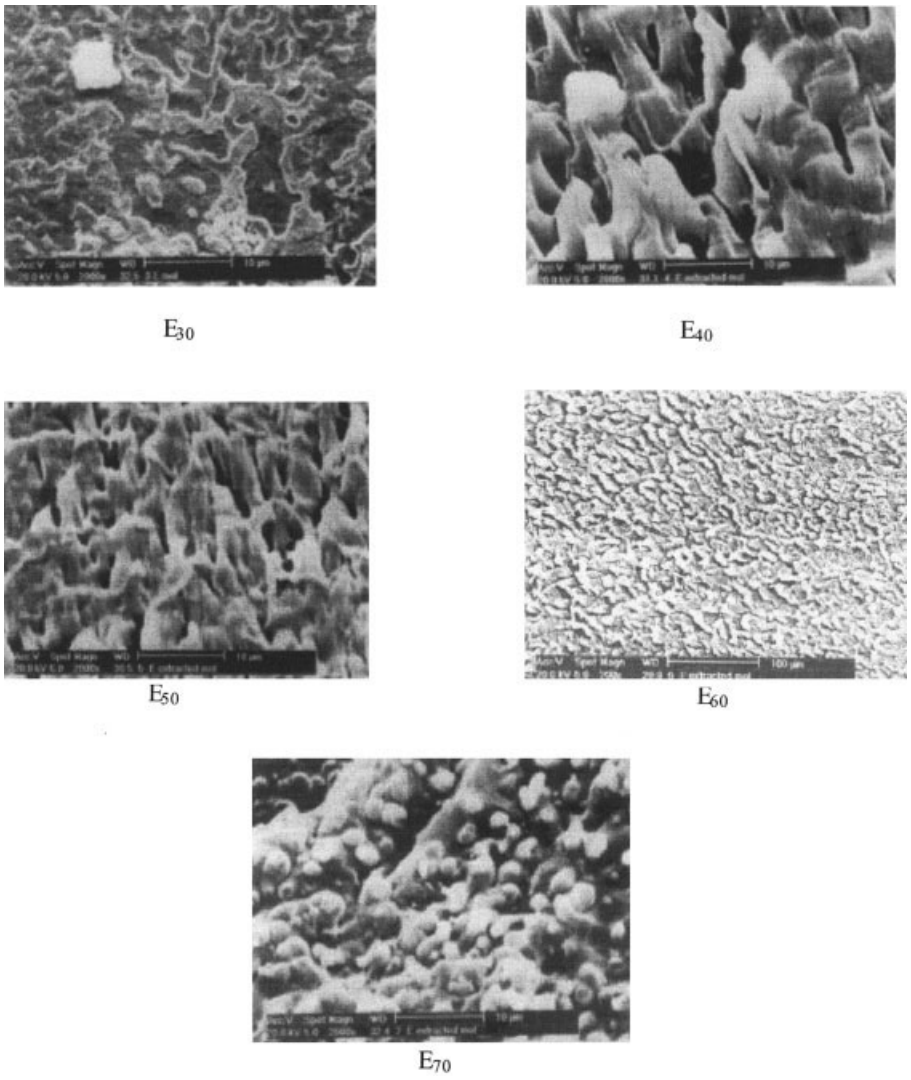

Figure 1 SEM micrographs of LLDPE/EVA blends.

were designated E_x (x = 0, 30, 50, 70, or 100), where x represents the weight percentage of EVA in the blend (with a view toward developing blends of thermoplastic elastomeric compositions, we are interested in 30/70, 50/50, and 70/30 EVA/LLDPE ratios). The compatibilized 70/30 LLDPE/EVA blends with 0, 0.5, 1, 3, and 5 wt % maleic-modified compatibilizer are represented as E_{30}, 0.5MC, 1MC, 3MC, and 5MC, respectively. The 70/30 LLDPE/EVA blends with the phenolic-modified compatibilizer are designated 0.5PC, 1PC, 3PC, and 5PC.

Morphology studies

Samples for scanning electron microscopy (SEM) analysis were prepared by the cryogenic fracturing of the samples in liquid nitrogen. To enhance morphological features and to facilitate easy identification of phases, the cryogenically fractured samples were etched with CCl_4 to extract the minor EVA phase. The dried samples were sputter-coated with gold and scanned under a scanning electron microscope.

Selective-solvent extraction

A selective-solvent dissolution technique was used to determine the cocontinuity region. The selected solvent used to dissolve the EVA phase was chloroform. No solvent was available for LLDPE. An approximately 1 g sample was weighed and immersed in 250 mL of the solvent for 10 days at room temperature. After 10 days, the solvent was changed to allow better dissolution of the considered phase. After 5 days, the remaining parts of the sample were dried in vacuo at 40°C and then weighed again.

DMA

The viscoelastic properties of the blends were measured with a Polymer Laboratories MK-II dynamic

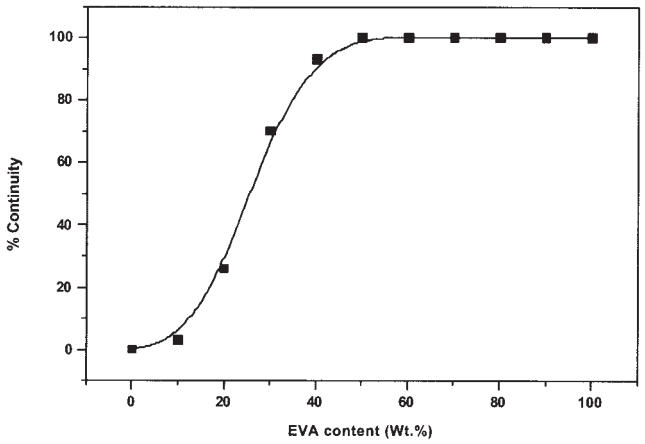

Figure 2 Effect of the blend composition on the cocontinuity.

mechanical thermal analyzer at a dynamic tension strain amplitude of 0.325% in the tensile mode at a frequency range of 0.1–50 Hz. The temperature of the testing was −60 to 35°C. Compression-molded samples ($70 \times 12 \times 5$ mm^3) were used for testing.

RESULTS AND DISCUSSION

Morphology and dynamic mechanical properties of the uncompatibilized blends

The SEM micrographs of the blends E_{30}, E_{40}, E_{50}, E_{60}, and E_{70} are shown in Figure 1. They demonstrate a two-phase morphology. From the photographs, it is clear that, up to E_{30}, EVA is dispersed as spherical domains in a continuous LLDPE matrix. When the proportion of EVA is 40%, there is onset of cocontinuity. An interpenetrating cocontinuous morphology is obtained for the 50/50 EVA/LLDPE system. By the addition of 60% EVA, the cocontinuous morphology slightly changes, and beyond E_{60}, EVA forms a continuous phase, and LLDPE is dispersed in it.

The results from the selective-solvent dissolution technique were also used to determine the cocontinuity region. The continuity of one phase can be defined as the fraction of the polymer that belongs to a continuous phase. For polymer A, this parameter is evaluated with the following expression:

$$\text{Continuity of A (\%)} = \frac{m_{\text{initial}}(\text{sample}) - m_{\text{final}}(\text{sample})}{w(\text{A}) \times m_{\text{initial}}(\text{sample})} \times 100 \quad (1)$$

where m_{initial} is the mass of sample before extraction, m_{final} is the mass of sample after extraction, and w(A) is the weight fraction of A in the initial blend. When the percentage of continuity of both components equals 100%, the morphology of the blend is considered to be cocontinuous. From selective dissolution experiments, a continuity diagram has been drawn, and above 40 wt % EVA, the EVA phase is continuous (Fig. 2). The sample after extraction did not break down (disintegrate) between 0 and 60 wt % EVA, and this indicates that the LLDPE phase is continuous in that range.

The dynamic mechanical properties, that is, E', E'', and damping (tan δ), of the pure components and blends were evaluated from −60 to + 35°C. Figure 3 shows the variation of tan δ with the temperature for the pure components and blends. Various researchers[20–23] have used dynamic mechanical investigation to predict the miscibility of polymeric systems. Generally, for an incompatible system, the tan δ–temperature curve shows two tan δ or damping peaks corresponding to the T_g's of individual polymers. In blends of any two polymers in the amorphous state, the presence of a single T_g intermediate between those of the pure polymers confirms the miscibility of the systems. A highly compatible blend shows only a single peak between the transition temperatures of the component polymers; whereas broadening of the transition occurs in the case of partially compatible systems. Shifted T_g's are also indicative of partial miscibility. In Figure 3, EVA shows a sharp peak. Because of the interaction between EVA and LLDPE, we get a broad peak for the EVA phase in the blends. The broadness of the peaks is an indication of an interaction between the components. There is some interaction between the two polymers on account of the similarity of the structures

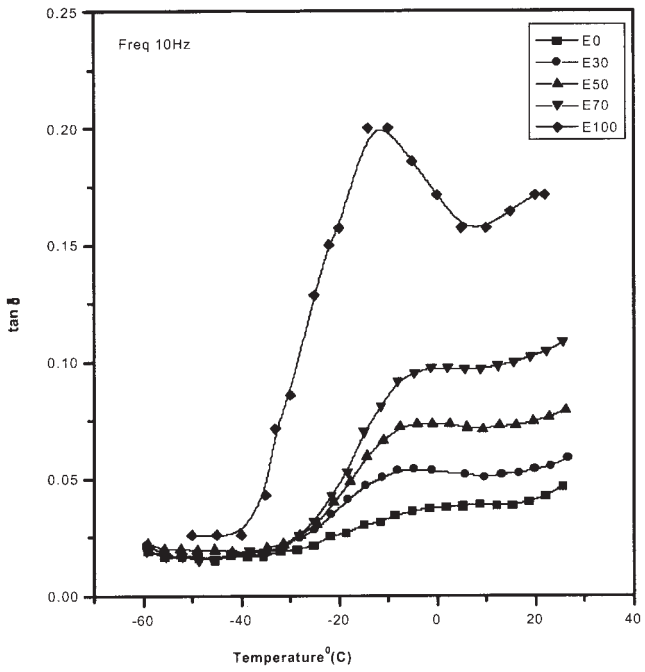

Figure 3 Effect of the temperature on the tan δ values of LLDPE/EVA blends.

TABLE III
***E* for the Transition of the EVA Phase in the LLDPE/EVA Blends**

Sample	*E* (J/mol)
E_{100}	1.4
E_{70}	1.1
E_{50}	1.41
E_{30}	1.1

between EVA and LLDPE. EVA contains polyethylene segments. Therefore, these segments are compatible with the LLDPE phase. As a result, T_g is shifted. However, the resolution of T_g analysis is limited to 10-nm scales. In the case of compatible and partially compatible blends, the T_g values are shifted to higher or lower temperatures, depending on the composition. There are primary and secondary relaxations in the case of polymers. The primary relaxations include melting and phase changes. During secondary relaxations, the heat capacity changes, but no phase change occurs. The α, β, and γ relaxations are secondary relaxations, and α is the glass-transition change. In the case of LLDPE/EVA blends, there is a transition corresponding to T_g of EVA. We can expect a transition corresponding to T_g of LLDPE also, which we could not detect in the set experimental temperature range. The tan δ curve of EVA at 10 Hz shows a peak at -12°C due to the α transition arising from the segmental motion of EVA, which corresponds to T_g of EVA. LLDPE has a relaxation at 0°C in the tan δ–temperature curve. This relaxation corresponds to the β relaxation of LLDPE, which is associated with the relaxation of small side groups in the amorphous region. The α transition of LLDPE is at a very low temperature that we could not detect in our experimental temperature range. EVA has shown high damping because of its rubbery nature. As the EVA content decreases, tan δ decreases. In the case of blends, T_g shifts toward a higher temperature region. Such a shift is similar to the effects of fillers on T_g of polymers. T_g of EVA shifting toward the right in the presence of LLDPE is due to the presence of crystallinity in LLDPE. Here crystallites are acting as fillers. WAXS results also support the increase in the crystallinity of blends in the presence of LLDPE.[24]

The activation energy (E) values for the glass transition due to the EVA phase of the blends have been calculated with an Arrhenius equation:

$$\log f = \log A - E/RT \tag{2}$$

where f is the frequency of the transition, A is the pre-exponential factor, R is the universal gas constant, and T is the temperature (K). The plots of log f versus $1/T$ were constructed, and the E values were calculated from the slopes of the plots. The E values for the transition of EVA are given in Table III. The blends E_{30} and E_{70} show lower E values because of the incompatible two-phase morphology. The blend E_{50} has the highest E value because of its cocontinuous morphology, which provides more interactions between the two phases.

Phase mixing in the blends

The fundamental nature of damping in polymers originates from the coordinated chain motion associated with the relaxation process, especially the glass transition. As the temperature or frequency is varied, E'' and tan δ exhibit peaks at which damping reaches a maximum. The areas under the linear tan δ–temperature (tan δ area) and linear E''–temperature [loss area (LA)] curves can be characterized to develop a relationship between the damping and molecular architecture. The area under the E''–temperature curves (LA) is related to the chemical composition of the material. The quantity LA was found to be a molecular characteristic governed by the structure of the individual polymers.

The integral of the E''–temperature curve is characterized to develop a relationship between the extent of damping and the contribution for each group toward the damping performance. Sperling et al.[25] suggested five methods to evaluate the area under the linear E''–temperature curve (LA). Of those methods, we made use of the integral method. The area under the linear E''–temperature curve can be derived with the phenomenological approach:[26]

$$\mathrm{LA} = \int_{T_G}^{T_R} E''\, dT \cong (E'_G - E'_R)\,\frac{R}{(E_a)_{\mathrm{avg}}}\,\frac{\pi}{2}\,T_g^2 \tag{3}$$

where E'_G and E'_R are the storage moduli in the glassy and rubbery states and T_G and T_R are the glassy and rubbery temperatures just below and above the glass transition, respectively. $(E_a)_{\mathrm{avg}}$ is the activation energy of the relaxation process, and R is the gas constant.

The group contribution analysis method is used to determine the theoretical values of LA. It is based on the assumption that the structural groups in the repeating units provide a weight fraction additive contribution to the total LA. The basic equation for the group contribution analysis of LA is[26,27]

$$\mathrm{LA} = \sum_{i=1}^{n} \frac{(\mathrm{LA})_i M_i}{M} = \sum_{i=1}^{n} \frac{E_i}{M} \tag{4}$$

where M_i is the molecular weight of the ith group of the repeating unit, M is the molecular weight of the whole mer, E_i is the molar loss constant for the ith

TABLE IV
Theoretical and Experimental values of *LA*

Sample	Experimental *LA* (GPa K)	Theoretical *LA* (GPa K)
E_{30}	21.31	3.70
E_{50}	14.48	3.98
E_{70}	3.82	4.26

group, and n represents the number of moieties in the mer. Equation (4) provides a predictive method for LA values via the structure of the polymer.

The theoretical and experimental values of LA for various blends are given in Table IV. The experimental values are larger than those obtained by group contribution analysis. This is because the experimental value of LA is influenced by the morphology, the interaction between the polymer components, and the phase continuity of the system. The higher experimental values of LA indicate enhanced interactions between the component polymers and enhanced damping. In the case of LLDPE/EVA blends, there will be some sort of borderline compatibility that may arise because of the structural similarity of LLDPE and EVA.

Theoretical modeling of the dynamic mechanical properties

The applicability of various composite models, such as the parallel, series, Halpin–Tsai, Corans, and Takayanagi models, are examined to predict the dynamic mechanical behavior of the blends. The parallel model (highest upper bound model) is given by the following equation:[28]

$$M = M_1\phi_1 + M_2\phi_2 \tag{5}$$

where M is the property of the blend; M_1 and M_2 are the corresponding properties of components 1 and 2, respectively; and ϕ_1 and ϕ_2 are the volume fractions of components 1 and 2, respectively. In this model, the components are considered to be arranged parallel to one another so that the applied load stretches each of the component by the same amount.

In the lower bound series model, the components are arranged in series with the applied stress. The equation is[28]

$$1/M = \phi_1/M_1 + \phi_2/M_2 \tag{6}$$

According to the Halpin–Tsai equation[29,30]

$$M_1/M = (1 + A_iB_i\phi_2)/(1 - B_i\phi_2) \tag{7}$$

$$B_i = (M_1/M_2 - 1)/(M_1/M_2 + A_i) \tag{8}$$

In this equation, subscripts 1 and 2 refer to the continuous and dispersed phases, respectively. The constant A_i is defined by the morphology of the system. For elastomer domains dispersed in a hard continuous matrix, A_i is 0.66, and for hard domains dispersed in an elastomeric matrix, A_i is 1.5.

The properties of an incompatible blend usually are between the upper bound parallel model (M_U) and the lower bound series model (M_L). According to Coran's equation[31]

$$M = f(M_U - M_L) + M_L \tag{9}$$

where f can vary between zero and unity. The value of f is given by

$$f = V_H^n(nV_S + 1) \tag{10}$$

where n contains the aspects of phase morphology. V_H and V_S are the volume fractions of the hard phase and soft phase, respectively.

The viscoelastic behavior of heterogeneous polymer blends can be predicted with Takayanagi's model. The Takayanagi model is given by[32]

$$E = (1 - \lambda)E_M + [(1 - \phi)/E_M) + (\phi/E_N)]^{-1} \tag{11}$$

where E_M is the complex modulus of the matrix phase, E_N is the complex modulus of the dispersed phase, and $\lambda\phi$ is the volume fraction of the dispersed phase. The values of λ and ϕ are related to the degree of series–parallel coupling.

The degree of parallel coupling of the model can be expressed by[10]

$$\%\ \text{parallel} = [\phi(1 - \lambda)/(1 - \lambda\phi)] \times 100 \tag{12}$$

Figure 4 shows the experimental (at 0°C) and theoretical plots of E' of LLDPE/EVA blends as a function of the volume fraction of EVA in the blend. The modulus decreases as the concentration of EVA increases. The curve shows a positive deviation from the additivity line, and this may be correlated to the morphology of the system. The blends E_{40} to E_{60} have a cocontinuous morphology, which contributes to the E' value. The curve shows a slope change from E_{60} to E_{100}, which is attributed to phase inversion of EVA. Among the different theoretical models, Coran's model is close to the experimental values.

Effect of compatibilization

By the addition of a suitably selected compatibilizer to immiscible blends, the interfacial tension can be re-

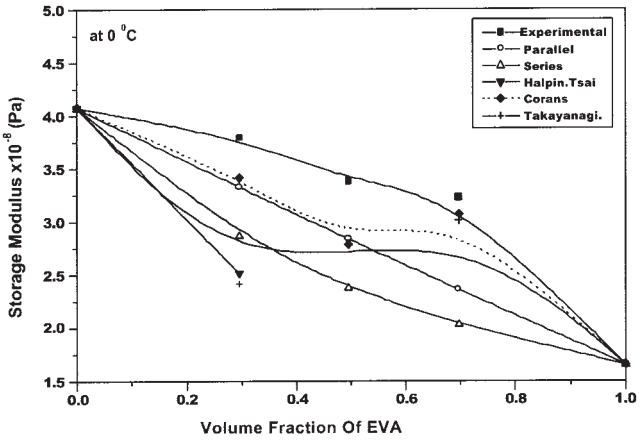

Figure 4 Applicability of various theoretical models for predicting E' of LLDPE/EVA blends.

duced, and a finer dispersion of the dispersed phase is achieved during mixing. Above all, it provides good interfacial adhesion.[33] The physical properties of polymer blends are highly affected by the morphology of the compatibilized blends.[34–36] According to brush theory, the interdiffusion between neighboring polymers resulting in the entanglement of polymer chains is of great importance for bonding between phases.[37,38] The presence of compatibilizers increases the interfacial thickness, and this effect is related to the molecular weight of the surface-attached compatibilizer.[39] The thickest interface was observed for the compatibilizer having the highest molecular weight. When the length of fully stretched compatibilizer chains are compared to the thickness of the interfaces, the interfaces are found to be thicker than the length of the compatibilizer chains.[40] This observation points to the fact that the compatibilizer chains restrict the mobility of the matrix chains with which they are not in direct contact. There may be a probable stretching of the compatibilizer chains away from the matrix, forming a brushlike structure, which can be schematically represented as shown in Figure 5. The hydrophobic LLDPE chains of the compatibilizer prefer to interact with the LLDPE matrix and are repelled by the polar EVA phase. The polar MA part of the compatibilizer interacts with the EVA phase.

The roles of phenolic-modified LLDPE and maleic-modified LLDPE as compatibilizers in LLDPE/EVA blends have also been investigated and compared. The mechanism of the modification of LLDPE by the grafting of MA is presented in Figure 6(a). The grafting reaction is carried out by a melt mixing technique at 125° C and at 60 rpm. The mixing time is 6 min. In the presence of dicumyl peroxide, free radicals are generated, which in turn generate free radicals from polyethylene, which is grafted to MA. As the MA group is polar in nature, when we use it as a compatibilizer, there will be polar/polar interactions between the polar EVA and MA group in the compatibilizer. The nonpolar polyethylene part of the compatibilizer goes with the LLDPE phase. The expected mechanism of compatibilization of LLDPE/EVA blends with phenolic resin (Ph)-g-LLDPE is given in Figure 6(b). Here also there are polar/polar interactions between the vinyl acetate group in EVA and the hydroxyl group in Ph–LLDPE. Upon the addition of these compatibilizers, the interfacial thickness increases, and this leads to effective stress transfer between the dispersed phase and the continuous phase, an increase in the interfacial adhesion, and a reduction in the interlayer slip.

Morphology and dynamic mechanical properties of the compatibilized blends

The effects of phenolic-modified polyethylene and maleic-modified polyethylene as compatibilizers on the morphology of E_{30} blends are presented in Figures 7 and 8, respectively. From the SEM micrographs, it is clear that the size of the dispersed EVA domains is reduced by the addition of the compatibilizers. Similar behavior was observed for other blend compositions. This reduction in the domain size of dispersed EVA upon the addition of MA-*g*-LLDPE and Ph–LLDPE is due to the reduction in the interfacial tension between the dispersed EVA phase and LLDPE matrix and the suppression of coalescence, which results in the stabilization of the blend morphology. In addition, the presence of the graft copolymer at the blend interface broadens the interfacial region through the penetration of the copolymer chain segments into the corresponding adjacent phases.[41] The average domain size of the compatibilized blends as a function of the compatibilizer concentration is given in Figure 9. The average domain diameter of the uncompatibilized E_{30} blend is 3.44 μm. In the case of compatibilized blends,

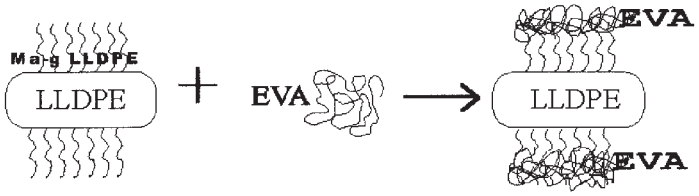

Figure 5 Schematic representation of the brush theory of compatibilization.

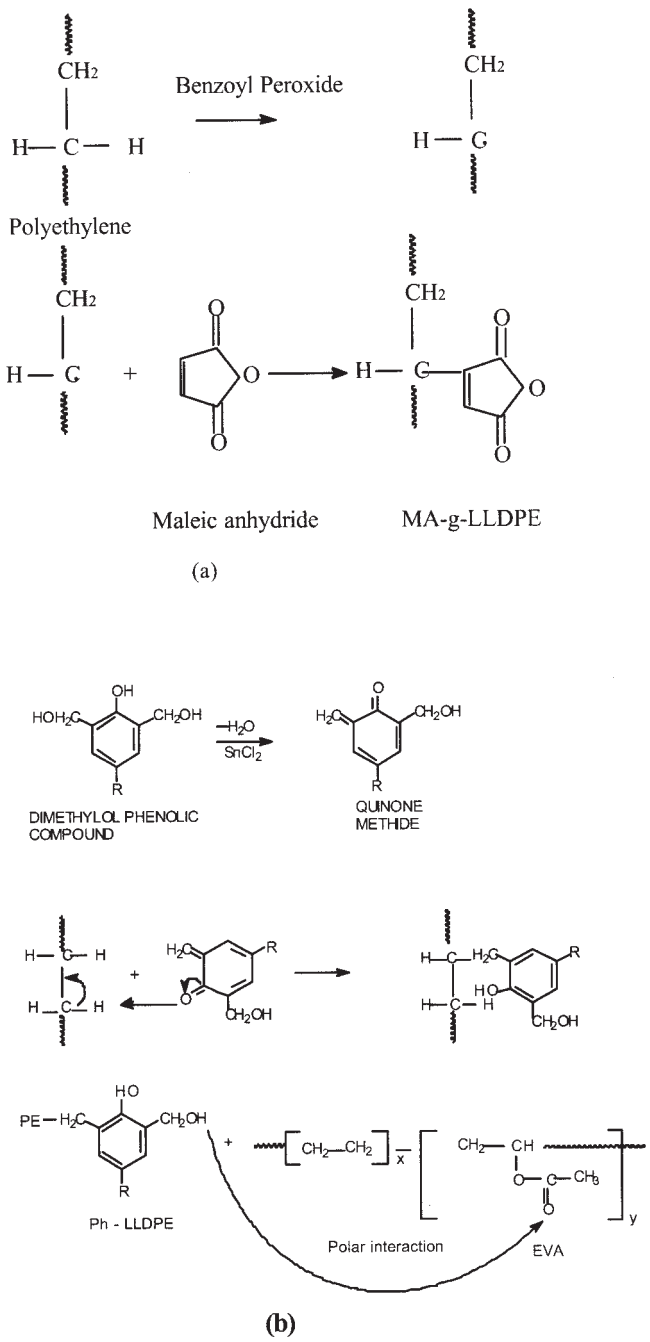

Figure 6 (a) Probable modification of LLDPE in the presence of MA and (b) probable mechanism of compatibilization of LLDPE/EVA blends in the presence of Ph-*g*-LLDPE.

the addition of 0.5% MA-*g*-LLDPE compatibilizer reduces the domain size to 1.2 μm, thereby causing a reduction in size up to 64%. Up to 0.5% MA-*g*-LLDPE, a reduction in the domain size can be noticed. Beyond this concentration, MA-*g*-LLDPE causes a slight increase in the size of the dispersed domain and then levels off, possibly because of micelle formation in the continuous polyethylene matrix. The addition of Ph–LLDPE up to a 3% concentration reduces the domain size, and a slight increase in the domain size can be observed with an increase in the concentration of Ph–LLDPE. The equilibrium concentration at which the domain size levels off can be considered the so-called critical micelle concentration (cmc), that is, the concentration at which micelles are formed. The cmc has been estimated by the intersection of the straight lines at the low- and high-concentration regions.[34–36] The cmc value for MA-*g*-LLDPE is 0.5%. The cmc value indicates the critical amount of compatibilizer required to saturate the unit of volume of the interface. Generally, cmc is estimated from a plot of the interfacial tension versus the copolymer concentration. As the interfacial tension is directly proportional to the domain size, cmc can be estimated from a plot of the domain size versus the copolymer concentration.[42] Several studies have been reported on interfacial saturation by the addition of compatibilizers.[43–47] This study and almost all the reported studies on the physical and reactive compatibilization of immiscible polymer blends and the theoretical prediction of Noolandi and Hong[48–50] suggest that a critical concentration of the compatibilizer is required to saturate the interface of binary polymer blends. Above this critical concentration, the compatibilizer may not modify the interface but forms micelles in the bulk phase.

One can also explain the interfacial saturation based on Taylor's theory.[51,52] In Taylor's theory, the particle size and the critical Webber number (W_e) are related by the following equation:

$$W_e = G\eta_m D/\gamma \tag{13}$$

where G is the shear rate, η_m is the matrix viscosity, D is the domain size of the dispersed phase of the blend, and γ is the interfacial tension of the blend. Upon the addition of the compatibilizer, the interfacial tension decreases, and there is a consequent particle breakdown. However, at a particular compatibilizer loading, there is a balance of interfacial tension and shear stress. From the equation, it is clear that there is a critical value of W_e below which no particle breakdown occurs and hence a critical particle size. At this point, the compatibilizer attains the highest possible interfacial area, and therefore there must be a maximum quantity of the compatibilizer required to saturate the blend interface. According to Tang and Huang,[53] the average radius (R) of the dispersed phase is given by

$$R = (R_0 - R_S)e^{-KC} + R_S \tag{14}$$

where R_0 and R_s are the average radii of dispersed domains at a compatibilizer concentration if zero and at saturation, respectively, and C is the concentration of the compatibilizer. The equation is based on the

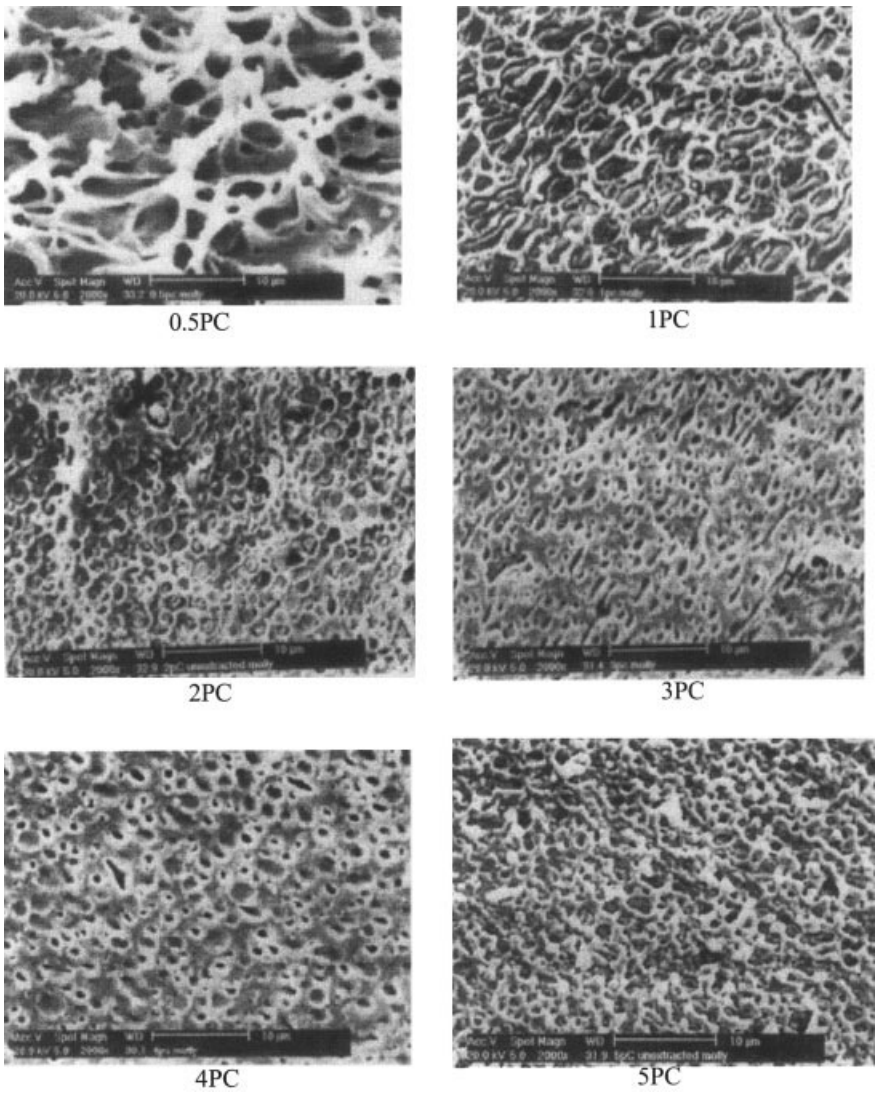

Figure 7 SEM micrographs of Ph–LLDPE-compatibilized E_{30} blends.

assumption that the change in the interfacial tension with the concentration of compatibilizer is given by

$$-d\gamma/dc = K(\gamma - \gamma_s) \tag{15}$$

where γ is the interfacial tension at compatibilizer concentration C, γ_s is the interfacial tension at the saturation concentration, and K is a constant. The changes in the average radius of domains with the compatibilizer concentration were fitted to eq. (14), and the values of K were determined and plotted against the compatibilizer concentration in Figure 10. The K value is expected to increase with the level of compatibilization and decrease with the degree of self-association in the blend.[53,54]The figure is in agreement with the theory. In the case of MA-*g*-LLDPE, K increases up to about 0.5 wt % compatibilizer, whereas in the case of Ph-*g*-LLDPE, K increases up to 3 wt % and then decreases with a further increase in the compatibilizer concentration; this depicts the saturation of the interface followed by micelle formation.

The area occupied by MA-*g*-LLDPE at the blend interface, Σ, was calculated with the expression suggested by Paul and Newman:[55]

$$\Sigma = 3\phi_A M/mRN \tag{16}$$

where M is the molecular weight of the copolymer, N is Avogadro's number, ϕ_A is the volume fraction of homopolymer A in an A/B blend, R is the radius of the dispersed domains, and m is the mass of the copolymer required to saturate the unit of volume of the blend interface (cmc).

On the basis of the values of Σ, one can deduce the conformation of the graft copolymer at the blend interface. There are two physical models showing the conformation of the compatibilizer molecule at the interface. In the first model, the blocks of the copoly-

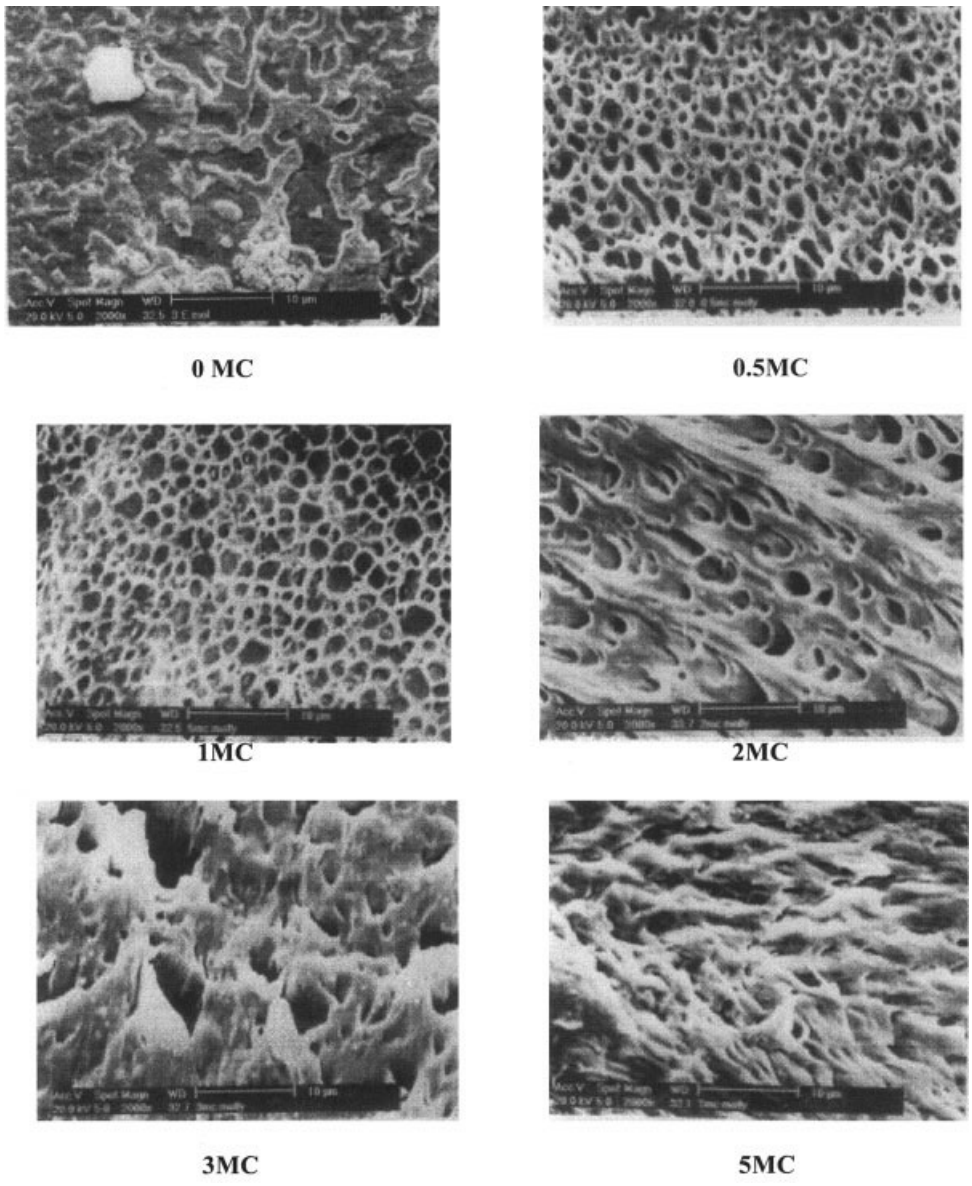

Figure 8 SEM micrographs of MA-*g*-LLDPE-compatibilized E_{30} blends.

mer extend to the corresponding homopolymer phase, as shown in Figure 11(a). In such a case, the area occupied by the copolymer at the interface is the cross-sectional area of the extended copolymer molecule, and this value is found ~0.5 nm^2. In the second model, the copolymer is believed to lie almost completely flat at the interface [Fig. 11(b)]. In this case, the occupied area will be the lateral surface area of the entire copolymer molecule. This has been estimated on the basis of the root mean square radius of gyration of the compatibilizer, and the value is close to 112 nm^2. The Σ values for various concentrations of MA-*g*-LLDPE for the 70/30 LLDPE/EVA blend have been calculated. At about 0.5% MA-*g*-LLDPE, the copolymer attains the maximum interfacial area. The value of the interfacial area of the compatibilizer at the blend in-

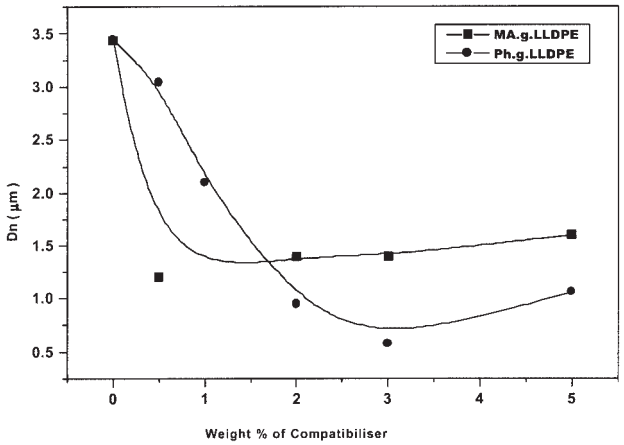

Figure 9 Effect of the compatibilizer concentration on the dispersed domain diameter (D_n) of E_{30} blends.

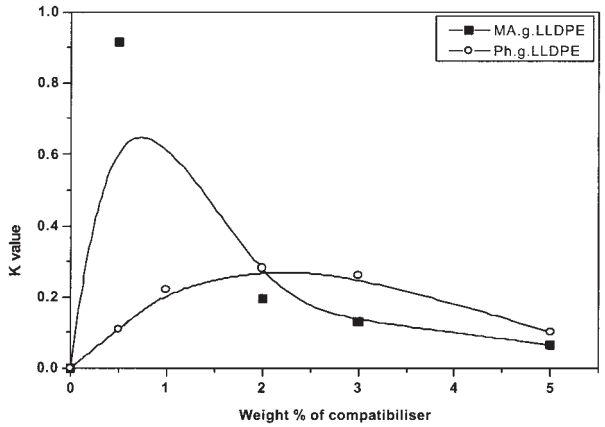

Figure 10 Effect of the compatibilizer concentration on the K value.

terface at cmc is 3.18 nm^2. This value is intermediate between the fully extended model (0.5 nm^2) and the flat model (112 nm^2). Therefore, it is reasonable to believe that the conformation of the compatibilizer at the blend interface is an intermediate conformation, as shown in Figure 11(c).

Noolandi and Hong[48–50] proposed a general theory for two immiscible homopolymers, A and B, diluted with a solvent in the presence of a diblock copolymer. The authors derived the mean field equations for the fundamental probability distribution function for the system. The polymer density profile in the interfacial region was obtained by the solution of the mean field equation by numerical analysis. The interfacial tensions in these systems were evaluated on the basis of free energy considerations. Their model is based on the assumption that the part of the copolymer that does not localize the interface will be randomly distributed in the bulk of the homopolymers phase as micelles. Localization of the copolymer, however, results in a decrease in the entropy and ultimately limits the amount of the copolymer at the interface. The separation of the blocks and the consequent stretching of the blocks into the corresponding homopolymers also cause a decrease in entropy. However, the main contribution to the reduction in interfacial tension is the entropy loss of the copolymer that localizes at the interface. Noolandi and Hong, by neglecting the conformational entropy, derived an analytical expression for the interfacial tension reduction:

$$\Delta\nu = d\phi_c[(1/2\chi\phi_p + 1/Z_c) - 1/Z_c \exp(Z_c\chi\phi_p/2)] \quad (17)$$

where ϕ_c is the bulk copolymer volume fraction of the copolymer, ϕ_p is the bulk volume fraction of polymer A or B, Z_c is the degree of polymerization of the copolymer, and χ is the Flory–Huggins interaction parameter between A and B segments. Noolandi and Hong[50] further suggested that both the copolymer molecular weight and concentration are equally important in reducing the interfacial tension. They noted that the interfacial tension surface is bounded by a cmc curve, as blocks of large molecular weight tend to form micelles in the bulk of the homopolymer phases. Therefore, the theoretical treatment of Noolandi and Hong is valid only for concentrations below cmc. For concentrations below cmc, the interfacial tension is expected to decrease with the copolymer concentration, whereas for concentrations above cmc, a leveling off is expected. Noolandi[56] further suggested that in the absence of a solvent, eq. (16) could be reduced to

$$\Delta\nu = d\phi_c[(1/2\chi + 1/Z_c) - 1/Z_c \exp(Z_c\chi/2)] \quad (18)$$

Although the theory was developed for the action of a symmetrical diblock copolymer, A-*b*-B, in incompatible binary blends (A/B), it can be very well applied to other systems in which the compatibilizing action is not strictly by the addition of block copolymers.[35,45] As the interfacial tension reduction is directly proportional to the particle size reduction at a low volume fraction of the dispersed phase, as suggested by Wu,[57] it can be argued that

$$\delta D = K\, d\phi_c[1/2\chi + 1/Z_c \exp(Z_c\chi/2)] \quad (19)$$

where K is a proportionality constant.

A plot of the domain size reduction as a function of the volume fraction of MA-*g*-LLDPE for the 30/70 EVA/LLDPE blend is shown in Figure 12. At a low MA-*g*-LLDPE concentration (below cmc), there is a drastic decrease in the domain diameter with an increase in the volume fraction of the graft copolymer, whereas at a higher concentration (above cmc), a leveling off can be observed in agreement with the predictions of Noolandi and Hong.[48–50]

Figure 13 depicts the variation of E' of 30/70 EVA/LLDPE blends compatibilized with different concentrations of Ph–LLDPE and MA-*g*-LLDPE. With the addition of the compatibilizer, E' increases. Beyond a particular concentration of the compatibilizer loading, E' slightly decreases and levels off. In the case of the Ph–LLDPE compatibilizer, a 1% loading shows the maximum E'. If there are better interaction and adhesion between the phases, E' should increase with the compatibilizer concentration. The better interaction

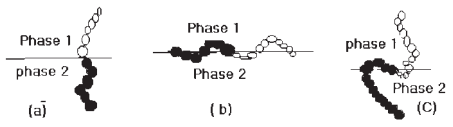

Figure 11 Schematic models illustrating the conformation of the copolymer at the interface.

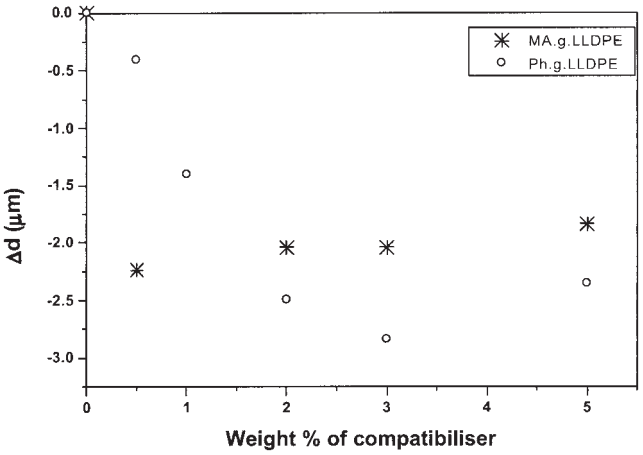

Figure 12 Variation of the particle size reduction (Δd) as a function of the weight percentage of the compatibilizer.

between LLDPE and EVA in the presence of Ph–LLDPE is evident from the SEM micrographs. However, a higher loading of the compatibilizer decreases the E' value because of micelle formation. This is in agreement with the morphological findings.

In the case of MA-*g*-LLDPE, the 0.5% compatibilizer loaded blend shows the highest E' value at various temperatures. In the interfacial modification of LLDPE/EVA with MA-*g*-LLDPE, the compatibilizer increases the interfacial interaction between EVA and LLDPE by the dipole/dipole interaction between the polar EVA part and polar MA part of MA-*g*-LLDPE. From the figure, it is clear that the maximum interfacial interaction is provided by a 0.5% compatibilizer loading, and beyond that loading, E' decreases and levels off because of micelle formation of the compatibilizer. From the SEM images, it is also clear that upon the addition of 0.5% compatibilizer, the morphology shows a fine and uniform distribution of the dispersed EVA phase, which provides maximum interaction between the phases.

Finally, we would like to comment on the role of the compatibilizer in the miscibility of the EVA/LLDPE polymer systems. Both electron microscopy and dynamic mechanical spectroscopy clearly show that the system is still phase-separated even in the presence of the compatibilizer. This is in agreement with Paul and Newman's[55] observation. According to Paul and Newman, if two polymers are far from being miscible, then no compatibilizer is likely to make a one-phase system. Therefore, for a completely immiscible system such as EVA/LLDPE, the main role of a compatibilizer is to act as an interfacial agent. By doing so, the interface is strengthened by the suppression of coalescence and reduction of interfacial tension. This in fact leads to a fine and stable morphology.

CONCLUSIONS

Morphology studies of LLDPE/EVA blends have revealed that the blends with a 40–60% composition have a cocontinuous morphology, and all other blends show a dispersed/matrix phase morphology. EVA-rich blends have LLDPE as the dispersed phase, and LLDPE-rich blends have EVA as the dispersed phase. The conformation of the compatibilizer in the interface is predicted by the calculation of the area occupied by the compatibilizer at the interface. The effects of the blend ratio and compatibilization on the dynamic mechanical properties of LLDPE/EVA blends have been analyzed in a temperature range of −60 to +35. The experimental E' values are higher than the theoretical E' values obtained by group contribution analysis, and this is an indication of some sort of interaction between the two phases. The tan δ curve of the blends shows a peak corresponding to the glass transition of EVA, which indicates that T_g of EVA is not affected by blending with LLDPE and points to the thermodynamic immiscibility of the blend system. The damping characteristics of the blend increase with increasing EVA content because of the decreasing crystalline volume of the system. Various composite models have been used to predict the dynamic mechanical data. Compatibilization increases the E' values of the system, and this is due to the fine dispersion of EVA domains in the LLDPE matrix providing increased interfacial interaction. The morphology of the blends has great influence on the viscoelastic properties. We have observed a very clear relationship between the morphology and dynamic mechanical spectroscopy. Very specifically, upon the addition of the compatibilizer, the domain size of the dispersed phase decreases and then levels off at a high concentration. The DMA analysis also indicates an increase in the E' values with the addition of a small amount of the compatibilizer, and a leveling off has been observed on account of interfacial saturation. Once the interface is saturated, the addition of more compatibilizer does not modify the interface anymore. This is reflected in the dynamic mechanical properties. Therefore, the

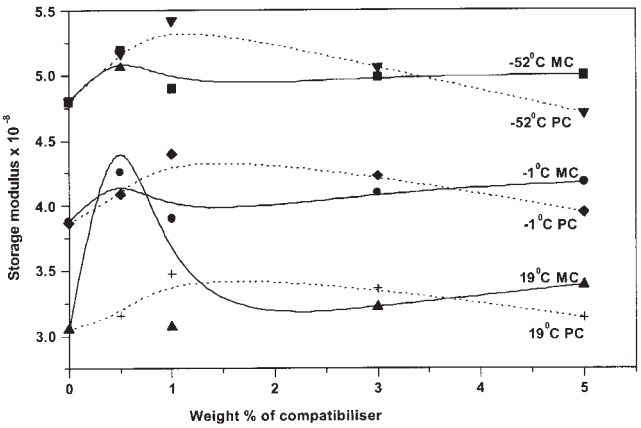

Figure 13 Effect of the compatibilizer concentration on E' of the E_{30} blend at different temperatures.

main contribution of this work is the interrelationship between the morphology and dynamic mechanical spectroscopy. We have also obtained a very good correlation with the compatibilization theories of Noolandi and Hong.[48–50]

References

1. Thermoplastic Elastomers from Rubber–Plastic Blends; De, S. K.; Bhowmick, A. K., Eds.; Ellis Horwood: New York, 1990.
2. Harris, B.; Braddel, O. G.; Almond, D. P.; Lefebvre, C.; Verbist, J. J Mater Sci 1993, 28, 3353.
3. Das, J.; Bandyopadhyay, S.; Blairs, S. J Mater Sci 1994, 29, 5680.
4. Wingard, C. D.; Beatty, C. L. J Appl Polym Sci 1990, 41, 2539.
5. Dynamic Mechanical Analysis of Polymeric Materials; Murayama, T. M., Ed.; Elsevier: New York, 1978.
6. Cho, K.; Ahn, T. K.; Lee, B. H.; Choe, S. J Appl Polym Sci 1997, 63, 1265.
7. Wippler, C. Polym Eng Sci 1990, 30, 17.
8. Jafari, S. H.; Gupta, A. K. J Appl Polym Sci 2000, 78, 962.
9. Oommen, Z.; Groeninckx, G.; Thomas, S. J Polym Sci Part B: Polym Phys 2000, 38, 582.
10. George, S.; Neelakantan, N. R.; Varughese, K. T.; Thomas, S. J Polym Sci Part B: Polym Phys 1997, 35, 2309.
11. John, J.; Mani, R.; Bhattacharya, M. J Polym Sci Part A: Polym Chem 2002, 40, 2003.
12. Cantor, A. S. J Appl Polym Sci 2000, 77, 826.
13. Akiyama, S.; Kobori, Y.; Sugisaki, A.; Koyama, T.; Akiba, I. Polymer 2000, 41, 4021.
14. Novikov, M. B.; Roos, A.; Creton, C.; Feldstein, M. M. Polymer 2003, 44, 3561.
15. Oulevey, F.; Burnham, N. A.; Gremaud, G.; Kulik, A. J.; Pollock, H. M.; Hammiche, A.; Reading, M.; Song, M.; Hourston, D. J. Polymer 2000, 41, 3087.
16. Cser, F.; Jollands, M.; White, P.; Bhattacharya, S. J Therm Anal Calorim 2002, 70, 651.
17. Moly, K. A.; Oommen, Z.; Bhagawan, S. S.; Groeninckx, G.; Thomas, S. J Appl Polym Sci 2002, 86, 3210.
18. Moly, K. A.; Bhagawan, S. S.; Thomas, S. Mater Lett 2002, 53, 346.
19. Coran, A. Y.; Patel, R. Rubber Chem Technol 1983, 56, 1045.
20. Varughese, K. T.; Nando, G. B.; De, P. P.; De, S. K. J Mater Sci 1988, 23, 3894.
21. Thomas, S.; George, A. Eur Polym 1992, 28, 145.
22. Walsh, D. J.; Higgins, J. S. Polymer 1982, 23, 336.
23. Thomas, S.; Gupta, G. R.; De, S. K. J Vinyl Technol 1987, 9, 71.
24. Moly, K. A.; Androsch, R.; Radhusch, H. J.; Bhagawan, S. S.; Thomas, S. Eur Polym J 2005, 41, 1410.
25. Fay, J. J.; Thomas, D. A.; Sperling, L. H. J Appl Polym Sci 1991, 43, 1617.
26. Chang, M. C. O.; Thomas, D. A.; Sperling, L. H. J Appl Polym Sci 1987, 34, 409.
27. Chang, M. C. O.; Thomas, D. A.; Sperling, L. H. J Polym Sci Part B: Polym Phys 1988, 26, 1627.
28. Thomas, S.; George, A. Eur Polym J 1992, 28, 1451.
29. Nielson, N. E. Rheol Acta 1974, 13, 86.
30. Halpin, J. Compos Mater 1970, 3, 732.
31. Coran, A. Y. In Hand Book of Elastomers: New Development and Technology; Bhomick, A. K.; Stephens, H. L., Eds.; Marcel Dekker: New York, 1988; p 249.
32. Holsti-Miettinen, R. M.; Seppala, J. V.; Ikkala, O. T.; Reima, I. T. Polym Eng Sci 1994, 34, 395.
33. Paul, D. R.; Barlow, G. W. Am Chem Soc Adv Chem Ser 1979, 176, 315.
34. Brahimi, B.; Ait-Kadi, A.; Ajji, A.; Fayt, R. J Polym Sci Part B: Polym Phys 1991, 29, 946.
35. Oommen, Z.; Gopinathan Nair, M. R.; Thomas, S. Polym Eng Sci 1996, 36, 151.
36. Asaletha, R.; Kumaran, M. G.; Thomas, S. Rubber Chem Technol 1995, 68, 671.
37. Brown, H. R.; Yang, A. C. M.; Russel, T. P.; Volksen, W.; Kramer, E. J. Polymer 1988, 29, 1807.
38. Yukioka, S.; Nagato, K.; Inoue, T. Polymer 1992, 33, 1171.
39. Felix, J. M.; Gatenholm, P. Am Chem Soc Polym Mater Sci Eng Div Proc 1992, 67.
40. Gatenholm, P.; Felix, J. M. In New Advances in Polyolefins; Chung, T. C., Ed.; Plenum: New York, 1993; p 237.
41. Dedecker, K.; Groeninck, G. Polymer 1998, 39, 4985.
42. Thomas, S.; Prud'homme, R. E. Polymer 1992, 33, 4260.
43. Willis, J. M.; Favis, B. D. Polym Eng Sci 1990, 30, 1073.
44. Cinaga, P.; Favis, B. D.; Jerome, R. J Polym Sci Part B: Polym Phys 1996, 34, 1691.
45. Kim, S. J. K.; Kim, S.; Park, C. E. Polymer 1997, 38, 2155.
46. Fayt, R.; Jerome, R.; Teyssie, P. Polym Eng Sci 1987, 27, 328.
47. Quin, C.; Yin, J.; Huang, B. Polymer 1990, 31, 663.
48. Noolandi, J. Polym Eng Sci 1984, 24, 70.
49. Noolandi, J.; Hong, K. M. Macromolecules 1982, 15, 482.
50. Noolandi, J.; Hong, K. M. Macromolecules 1984, 17, 1531.
51. Taylor, G. I. Proc R Soc London Ser A 1932, 138, 41.
52. Taylor, G. I. Proc R Soc London Ser A 1934, 146, 501.
53. Tang, T.; Huang, B. Polymer 1994, 35, 281.
54. Jannasch, P.; Wesslen, B. J Appl Polym Sci 1995, 58, 753.
55. Paul, D. R.; Newman, S. Polymer Blends; Academic: New York, 1978; Chapter 12.
56. Noolandi, J. Private communications; 1987, 129.
57. Wu, S. Polym Eng Sci 1987, 27, 335.